JOURNAL OF CHEMICAL & ENGINEERING DATA

ARTICLE

pubs.acs.org/jced

Thermodynamic Modeling of the Sulfuric Acid−Water−Sulfur Trioxide System with the Symmetric Electrolyte NRTL Model

Huiling Que,[†] Yuhua Song,[‡] and Chau-Chyun Chen*[,‡]

[†]AspenTech Limited, Pudong, Shanghai 201203, China

[‡]Aspen Technology, Inc., Burlington, Massachusetts 01803, United States

ABSTRACT: Thermodynamic modeling of the sulfuric acid−water−sulfur trioxide system is of great interest to the industry. The recently developed symmetric electrolyte NRTL activity coefficient model is applied to develop a comprehensive thermodynamic model for the sulfuric acid system over the whole concentration range from pure water to pure sulfuric acid to pure sulfur trioxide with temperature up to 773 K. The model takes into account partial dissociations of sulfuric acid and bisulfate ion, hydration of hydronium ion, decomposition of sulfuric acid to water and sulfur trioxide, and formation of disulfuric acid from sulfuric acid and sulfur trioxide in the concentrated sulfur trioxide region. Excellent matches between model correlations and available literature data are achieved for vapor−liquid equilibrium, osmotic coefficient, liquid phase speciation, heat of dilution, heat of mixing, heat of solution, and liquid heat capacity of the sulfuric acid−water−sulfur trioxide system.

INTRODUCTION

Sulfuric acid is the largest volume industrial chemical produced in the world. Process modeling and simulation of the sulfuric acid−water−sulfur trioxide system is frequently practiced in the industry due to its wide applications. Two recent applications of high importance are dew point calculation of flue gas in oxyfuel combustion and process design for sulfur−iodine cycle thermochemical decomposition of water for hydrogen production.[1] Accurate and comprehensive thermodynamic modeling of the sulfuric acid system is a prerequisite to meaningful process modeling, simulation, design, analysis, and optimization.[2] While extensive progress has been made in thermodynamic modeling for the sulfuric acid system, this task remains a tall challenge due to the complex solution chemistry and the highly nonideal liquid phase of the sulfuric acid system.

Recent studies in thermodynamic modeling of the sulfuric acid system include those of Bollas et al.,[3] Wang et al.,[4] and Clegg and Brimblecombe.[5] Applying a refined electrolyte NRTL activity coefficient model, Bollas et al.[3] investigated speciation and solution nonideality of the aqueous sulfuric acid at 298 K. Assuming a "constant" average hydration of the proton ion, they reported excellent matches to osmotic coefficient data, mean ionic activity coefficient data, and degree of dissociation of the bisulfate ion data. The Bollas et al. study did not cover other temperatures and other properties of interest, such as vapor−liquid equilibrium (VLE), heat of dilution, and heat capacity. Applying an extended UNIQUAC model, Wang et al.[4] reported a modeling study on VLE and speciation from 298 to 773 K and over the whole concentration range, i.e., from pure water to pure sulfuric acid and then to pure sulfur trioxide. They further showed that an explicit account of hydronium ion improved their model predictions with respect to the speciation data. However, the Wang et al. study did not present modeling results for calorimetric properties, did not account for the known species of disulfuric acid in the concentrated sulfur trioxide region, and did not include the speciation data in the determination of model parameters. Furthermore, their extension of the model to temperatures above 573 K requires a "special" modification in their treatment of standard state properties.

Applying an extended Pitzer model, Clegg and Brimblecombe[5] reported a thermodynamic model that was fitted to osmotic coefficients, electromotive force measurements, degrees of dissociation of the bisulfate ion, differential heats of dilution, heat capacities, freezing points, and tabulated partial molal enthalpies of water for aqueous sulfuric acid from (< 200 to 328) K and from (0 to 40) *m* acid (∼ 0.80 mass fraction sulfuric acid) at 101 325 Pa pressure. While the study yielded a self-consistent representation of activities, speciation, and thermal properties, it did not explicitly account for hydrations of the proton ion, did not cover VLE data, and did not cover the full ranges of acid concentration and temperature of interest to industry.

In this work, we aim to develop a comprehensive thermodynamic model for the sulfuric acid−water−sulfur trioxide system. In addition to taking into account explicitly the complex solution chemistry taking place in the sulfuric acid system, we apply the newly developed symmetric electrolyte NRTL model[6,7] to correlate available experimental data of all pertinent thermodynamic properties including VLE, speciation, osmotic coefficient, heat of dilution, heat of mixing, heat of solution, and liquid heat capacity from (273 to 773) K and over the entire concentration range, i.e., from pure water to pure sulfuric acid and then to pure sulfur trioxide. Using this approach successful correlation of all pertinent experimental data is achieved.

THERMODYNAMIC FRAMEWORK

Chemical Reactions. Rigorous thermodynamic modeling of electrolyte solutions requires proper representation of all chemical

Special Issue: John M. Prausnitz Festschrift

Received: September 14, 2010
Accepted: November 16, 2010
Published: February 02, 2011

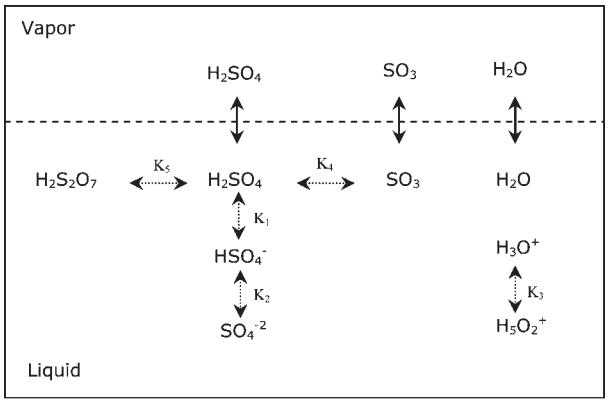

Figure 1. Solution chemistry and speciation in the sulfuric acid system.

reactions and resulting species.[8] In this study, we take full account of the complex solution chemistry taking place in the sulfuric acid system: (1) partial dissociations of sulfuric acid to bisulfate ion and sulfate ion in aqueous solution, (2) hydration of hydronium ion in aqueous solution, (3) decomposition of sulfuric acid to form sulfur trioxide in the concentrated sulfuric acid region, and (4) formation of disulfuric acid from sulfuric acid and sulfur trioxide in the concentrated sulfur trioxide region. These reactions are summarized in eqs R1 to R5.

$$H_2SO_4 + H_2O \overset{K_1}{\leftrightarrow} HSO_4^- + H_3O^+ \quad (R1)$$

$$HSO_4^- + H_2O \overset{K_2}{\leftrightarrow} SO_4^{-2} + H_3O^+ \quad (R2)$$

$$H_3O^+ + H_2O \overset{K_3}{\leftrightarrow} H_5O_2^+ \quad (R3)$$

$$SO_3 + H_2O \overset{K_4}{\leftrightarrow} H_2SO_4 \quad (R4)$$

$$SO_3 + H_2SO_4 \overset{K_5}{\leftrightarrow} H_2S_2O_7 \quad (R5)$$

Figure 1 depicts the resulting species from the reactions. There are four molecular species—water, sulfuric acid, sulfur trioxide, and disulfuric acid—and four ionic species—bisulfate ion, sulfate ion, hydronium ion (i.e., monohydrate of the proton ion), and dihydrate of the proton ion.

Reactions R1, R2, R4, and R5 are commonly known and covered in prior modeling studies.[2−4] Reaction R3, hydration of hydronium ion, is introduced in this work as recent studies[9,10] on hydrated protons revealed that both the monohydrate species (i.e., Eigen structure) and the dihydrate species (i.e., Zundel structure) represent the lowest energy state of the hydronium ion.

Experimental speciation studies for the oleum system were reviewed by Nilges and Schrage.[11] Besides sulfuric acid and sulfur trioxide, these speciation studies confirmed the presence of disulfuric acid in liquid phase and the presence of S_3O_9 in both liquid phase and vapor phase for highly concentrated oleum systems at temperatures below 373 K. Presence of polysulfuric acids, $H_2O(SO_3)_n$ with $n > 2$, were also detected by some studies but in small quantities. Nilges and Schrage further correlated the VLE data of Schrage[12] by incorporating three main species: sulfuric acid, sulfur trioxide and disulfuric acid. We follow the same treatment in this work. Due to the fact that disulfuric acid was not detected in vapor phase per review by Nilges and Schrage, disulfuric acid is treated as nonvolatile.

Vapor−Liquid Equilibrium. Vapor−liquid equilibrium for molecular species is described by the equality of component fugacity in liquid phase and in vapor phase:

$$P y_i \varphi_i = x_i \gamma_i f_i^0 \quad (1)$$

where P is the system pressure, y_i is the vapor phase mole fraction of component i, φ_i is the vapor phase fugacity coefficient of component i and calculated from the Redlich−Kwong equation of state, x_i is the liquid phase mole fraction of component i, γ_i is the liquid phase activity coefficient for component i and calculated from the symmetric electrolyte NRTL activity coefficient model,[6] and f_i^0 is the liquid fugacity of pure component i at the system temperature and pressure; it is also called the liquid phase reference fugacity and generally expressed as:

$$f_i^0 = P_i^0 \varphi_i^0 \theta_i^0 \quad (2)$$

where P_i^0 is the vapor pressure of pure component i at the system temperature $T$and calculated from the Steam Table equation of state[13] for water and the Antoine equation for sulfuric acid and sulfur trioxide, φ_i^0 is the vapor fugacity coefficient of pure component i at T and P_i^0, and θ_i^0 is the Poynting pressure correction from P_i^0 to P and assumed to be unity in this work.

Activity Coefficient Model. The symmetric electrolyte NRTL model[6] expresses excess Gibbs energy as the sum of two contributions:

$$G^{ex} = G^{ex,\,lc} + G^{ex,\,PDH} \quad (3)$$

where $G^{ex,lc}$ is the contribution from the short-range ion−ion, ion−molecule, and molecule−molecule interactions while $G^{ex,PDH}$ is the contribution from the long-range ion−ion interactions.

The short-range interactions that exist at the immediate neighborhood of any species are represented with the electrolyte NRTL local composition formulation:

$$\frac{G^{ex,\,lc}}{RT} = \sum_m n_m \left(\frac{\sum_i X_i G_{im} \tau_{im}}{\sum_i X_i G_{im}} \right) + \sum_c z_c n_c \left(\frac{\sum_{i \neq c} X_i G_{ic} \tau_{ic}}{\sum_{i \neq c} X_i G_{ic}} \right) + \sum_a z_a n_a \left(\frac{\sum_{i \neq a} X_i G_{ia} \tau_{ia}}{\sum_{i \neq a} X_i G_{ia}} \right) \quad (4)$$

$$X_i = C_i x_i = C_i \left(\frac{n_i}{n} \right), \quad i = \text{m, c, a} \quad (5)$$

$$n = \sum_i n_i = \sum_m n_m + \sum_c n_c + \sum_a n_a \quad (6)$$

$$G_{ij} = \exp(-\alpha_{ij} \tau_{ij}) \quad (7)$$

$$\tau_{ij} = \tau_{1,ij} + \frac{\tau_{2,ij}}{T} + \tau_{3,ij} \left(\frac{T^{ref} - T}{T} + \ln \frac{T}{T^{ref}} \right) \quad (8)$$

where R is the gas constant; i is the species index including molecular species m, cationic species c, and anionic species a; n_i and x_i are mole number and mole fraction of species i in the system, respectively; C_i is charge number for ionic species and unity for molecular species; α_{ij} is the nonrandomness factor; and τ_{ij} is the binary interaction energy parameter in which $\tau_{1,ij}$, $\tau_{2,ij}$, and $\tau_{3,ij}$ are parameters in the temperature correlation (eq 8) of τ_{ij} with T^{ref} = 298.15 K.

dx.doi.org/10.1021/je100930y |J. Chem. Eng. Data 2011, 56, 963–977

The long-range ion−ion interactions are represented with the extended Pitzer−Debye−Hückel (PDH) formula for multicomponent electrolytes:

$$\frac{G^{\mathrm{ex,\ PDH}}}{nRT} = -\frac{4A_\varphi I_x}{\rho}\ln\left[\frac{1+\rho I_x^{1/2}}{1+\rho(I_x^0)^{1/2}}\right] \tag{9}$$

with

$$A_\varphi = \frac{1}{3}\left(\frac{2\pi N_A}{v}\right)^{1/2}\left(\frac{Q_e^2}{\varepsilon k_B T}\right)^{3/2} \tag{10}$$

$$I_x = \frac{1}{2}\sum_i z_i^2 x_i = \frac{1}{2}\sum_c z_c^2 x_c + \frac{1}{2}\sum_a z_a^2 x_a \tag{11}$$

$$v = \frac{\sum_m x_m v_m}{\sum_m x_m} \tag{12}$$

$$\varepsilon = \frac{\sum_m x_m M_m \varepsilon_m}{\sum_m x_m M_m} \tag{13}$$

$$\varepsilon_m = A_m + B_m\left(\frac{1}{T} - \frac{1}{C_m}\right) \tag{14}$$

where A_φ is the Debye−Hückel parameter, I_x is ionic strength, ρ is the closest approach parameter, N_A is the Avogadro's number, k_B is the Boltzmann constant, I_x^0 is I_x at the fused salt reference state, and v and ε are the molar volume and dielectric constant of the mixed solvents, respectively. Both v and ε are calculated by the averages over all molecular solvent components in the solution. In eqs 12−14, v_m, M_m, and ε_m are molar volume, molecular weight, and dielectric constant of molecular solvent m, respectively; ε_m is correlated with T and three solvent-specific parameters A_m, B_m, and C_m in eq 14.

The activity coefficient of species i, γ_i, can be derived from excess Gibbs energy by

$$\ln\gamma_i = \frac{1}{RT}\left(\frac{\partial G^{\mathrm{ex}}}{\partial n_i}\right)_{T,\,P,\,n_{j\neq i}} \qquad i, j = m, c, a \tag{15}$$

Accordingly, the activity coefficients can also be written in two terms, the contribution from the short-range interactions, γ_i^{lc}, and the contribution from the long-range interactions, γ_i^{PDH}

$$\ln\gamma_i = \ln\gamma_i^{\mathrm{lc}} + \ln\gamma_i^{\mathrm{PDH}}, \quad i = m, c, a \tag{16}$$

Specifically, the normalized activity coefficients for molecular species m, cationic species c, and anionic species a can be derived as follows:

$$\ln\gamma_m^{\mathrm{lc}} = \frac{\sum_i X_i G_{im}\tau_{im}}{\sum_i X_i G_{im}} + \sum_{m'}\frac{X_{m'}G_{mm'}}{\sum_i X_i G_{im'}}\left(\tau_{mm'} - \frac{\sum_i X_i G_{im'}\tau_{im'}}{\sum_i X_i G_{im'}}\right) + \sum_c \frac{X_c G_{mc}}{\sum_{i\neq c} X_i G_{ic}}\left(\tau_{mc} - \frac{\sum_{i\neq c} X_i G_{ic}\tau_{ic}}{\sum_{i\neq c} X_i G_{ic}}\right) + \sum_a \frac{X_a G_{ma}}{\sum_{i\neq a} X_i G_{ia}}\left(\tau_{ma} - \frac{\sum_{i\neq a} X_i G_{ia}\tau_{ia}}{\sum_{i\neq a} X_i G_{ia}}\right) \tag{17}$$

$$\frac{1}{z_c}\ln\gamma_c^{\mathrm{lc}} = \sum_m \frac{X_m G_{cm}}{\sum_i X_i G_{im}}\left(\tau_{cm} - \frac{\sum_i X_i G_{im}\tau_{im}}{\sum_i X_i G_{im}}\right) + \frac{\sum_{i\neq c} X_i G_{ic}\tau_{ic}}{\sum_{i\neq c} X_i G_{ic}} + \sum_a \frac{X_a G_{ca}}{\sum_{i\neq a} X_i G_{ia}}\left(\tau_{ca} - \frac{\sum_{i\neq a} X_i G_{ia}\tau_{ia}}{\sum_{i\neq a} X_i G_{ia}}\right) \tag{18}$$

$$\frac{1}{z_a}\ln\gamma_a^{\mathrm{lc}} = \sum_m \frac{X_m G_{am}}{\sum_i X_i G_{im}}\left(\tau_{am} - \frac{\sum_i X_i G_{im}\tau_{im}}{\sum_i X_i G_{im}}\right) + \frac{\sum_{i\neq a} X_i G_{ia}\tau_{ia}}{\sum_{i\neq a} X_i G_{ia}} + \sum_c \frac{X_c G_{ac}}{\sum_{i\neq c} X_i G_{ic}}\left(\tau_{ac} - \frac{\sum_{i\neq c} X_i G_{ic}\tau_{ic}}{\sum_{i\neq c} X_i G_{ic}}\right) \tag{19}$$

$$\ln\gamma_i^{\mathrm{PDH}} = \frac{2A_\varphi I_x^{2/3}}{1+\rho I_x^{1/2}}, \quad i = m \tag{20}$$

$$\ln\gamma_i^{\mathrm{PDH}} = -A_\varphi\left\{\left(\frac{2z_i^2}{\rho}\right)\ln\left[\frac{1+\rho I_x^{1/2}}{1+\rho(I_x^0)^{1/2}}\right] + \frac{z_i^2 I_x^{1/2} - 2I_x^{3/2}}{1+\rho I_x^{1/2}} - \frac{2I_x(I_x^0)^{-1/2}}{1+\rho(I_x^0)^{1/2}}\left(n\frac{\partial I_x^0}{\partial n_i}\right)\right\}, \quad i = c, a \tag{21}$$

In the above equations for normalizing the activity coefficients, the symmetric reference state for ionic species is used. For a system containing only a single electrolyte component ca, the pure fused salt state can be defined as follows:

$$\gamma_{ca}(x_{ca}\to 1) = \gamma_\pm(x_{ca}\to 1) = 1 \tag{22}$$

For multielectrolyte systems, the symmetric reference state can be generalized from eq 22 as follows:

$$\gamma_{ca}(x_m\to 0) = \gamma_\pm(x_m\to 0) = 1 \tag{23}$$

where m applies to all molecular species in the system.

The reference state for a molecular species m is always defined as the standard state of pure liquid

$$\gamma_m(x_m\to 1) = 1 \tag{24}$$

Liquid Gibbs Free Energy, Enthalpy, and Heat Capacity Calculations. Liquid Gibbs free energy, enthalpy and heat capacity of the sulfuric acid system are related to activity coefficients. For instance, liquid enthalpy consists of contributions from pure component liquid enthalpies of each species and excess enthalpy. For molecular species, we compute the pure component liquid enthalpy from the ideal gas enthalpy and the enthalpy departure from the ideal gas state to the pure liquid phase. For ionic species, we compute the pure component liquid enthalpy from the enthalpy of the ideal fused salt state formed by the ion with all its counterions in the system. This enthalpy of fused salt can be thermodynamically related to the enthalpy of the ions at the aqueous phase infinite dilution state. The excess enthalpy is calculated from the activity coefficient model. Heat capacity is then calculated as the temperature derivative of enthalpy.

The liquid Gibbs free energy and enthalpy can be expressed, respectively, by the following equations:

$$G^{l} = RT \sum_{j=m,\,c,\,a} x_j \ln x_j + \sum_m x_m G_m^l + \sum_i x_i G_i^{\text{fused}} + G^{E},\ i = c,\ a \tag{25}$$

$$H^{l} = \sum_m x_m H_m^l + \sum_i x_i H_i^{\text{fused}} + H^{E},\quad i = c,\ a \tag{26}$$

$$G^{E} = RT\left(\sum_m x_m \ln \gamma_m + \sum_i x_i \ln \gamma_i\right),\quad i = c,\ a \tag{27}$$

$$H^{E} = -RT^2\left(\sum_m x_m \frac{\partial \ln \gamma_m}{\partial T} + \sum_i x_i \frac{\partial \ln \gamma_i}{\partial T}\right),\quad i = c,\ a \tag{28}$$

where G^{l} and H^{l} are the molar liquid Gibbs free energy and enthalpy of the solution, respectively, G_m^{l} and H_m^{l} are the molar liquid Gibbs free energy and enthalpy of molecular species m, respectively, G_i^{fused} and H_i^{fused} are the molar Gibbs free energy and enthalpy of ionic species i in the fused salt state (i.e., the symmetric reference state), respectively, and G^{E} and H^{E} are the excess Gibbs free energy and enthalpy of the solution, respectively.

The molar liquid Gibbs free energy and enthalpy of molecular species are calculated, respectively, by the following expressions:

$$G_m^{l} = G_m^{ig} + RT\ln(f_m^0/P^{\text{ref}}) \tag{29}$$

$$H_m^{l} = H_m^{ig} + \text{DHV}_m - \Delta_{\text{vap}}H_m \tag{30}$$

where G_m^{ig} and H_m^{ig} are the ideal gas Gibbs free energy and enthalpy and calculated from Aspen ideal gas model,[13] respectively, P^{ref} = 101325 Pa is the standard pressure, $\text{DHV}_m = H_m^{V} - H_m^{ig}$ is the vapor enthalpy departure and calculated from the Redlich−Kwong equation of state, and $\Delta_{\text{vap}}H_m$ is the heat of vaporization and calculated from Watson's equation.[13]

The molar Gibbs free energy and enthalpy of ionic species i in the fused salt state can be written, respectively, by the following equations:

$$G_i^{\text{fused}} = G_i^{\infty,\,\text{aq}} + \Delta G_i,\quad i = c,\ a \tag{31}$$

$$H_i^{\text{fused}} = H_i^{\infty,\,\text{aq}} + \Delta H_i,\quad i = c,\ a \tag{32}$$

where $G_i^{\infty,\text{aq}}$ and $H_i^{\infty,\text{aq}}$ are the aqueous phase infinite dilution Gibbs free energy and enthalpy of ionic species, respectively, and ΔG_i and ΔH_i are the Gibbs free energy and enthalpy corrections due to the change from the unsymmetrical reference state to the symmetric reference state, respectively.

To derive methods to calculate ΔG_i and ΔH_i, we apply the condition that the calculated liquid Gibbs free energy and enthalpy for the same electrolyte solution must be the same, respectively, regardless of the reference state specified for ionic species; that is

$$G^{l}(T,\ p, x_i) = G^{l,*}(T,\ p, x_i),\quad i = m,\ c,\ a \tag{33}$$

$$H^{l}(T,\ p, x_i) = H^{l,*}(T,\ p, x_i),\quad i = m,\ c,\ a \tag{34}$$

where $G^{l}(T,p,x_i)$ and $H^{l}(T,p,x_i)$are the liquid Gibbs free energy and enthalpy given by eqs 25 and 26, respectively, with the symmetric reference state for ionic species and $G^{l,*}(T,p,x_i)$ and $H^{l,*}(T,p,x_i)$ are the liquid Gibbs free energy and enthalpy, respectively, with the aqueous phase infinite dilution reference state for ionic species; they can be expressed as follows:

$$G^{l,*} = RT \sum_{j=m,\,c,\,a} x_j \ln x_j + \sum_m x_m G_m^{l} + \sum_i x_i G_i^{\infty,\,\text{aq}} + G^{E,*},\ i = c,\ a \tag{35}$$

$$H^{l,*} = \sum_m x_m H_m^{l} + \sum_i x_i H_i^{\infty,\,\text{aq}} + H^{E,*},\quad i = c,\ a \tag{36}$$

$$G^{E,*} = RT\left(\sum_m x_m \ln \gamma_m + \sum_i x_i \ln \gamma_i^{*}\right),\quad i = c,\ a \tag{37}$$

$$H^{E,*} = -RT^2\left(\sum_m x_m \frac{\partial \ln \gamma_m}{\partial T} + \sum_i x_i \frac{\partial \ln \gamma_i^{*}}{\partial T}\right),\quad i = c,\ a \tag{38}$$

where γ_i^{*} is the unsymmetrical activity coefficient of ionic species i with the aqueous phase infinite dilution reference state.

The condition given by eqs 33 and 34 holds at any state and we can apply it to the fused salt state of the solution, in which the compositions for all molecular species are zero. That is

$$x_m \to 0 \qquad \text{for all molecular species} \tag{39}$$

$$\gamma_i \to 1, i = c,\ a \quad \text{for all ionic species at the symmetric reference state} \tag{40}$$

We can then easily obtain these equations

$$G^{l}(T,\ p, x_i, x_m \to 0) = G^{l,*}(T,\ p, x_i, x_m \to 0),\quad i = c,\ a \tag{41}$$

$$H^{l}(T,\ p, x_i, x_m \to 0) = H^{l,*}(T,\ p, x_i, x_m \to 0),\quad i = c,\ a \tag{42}$$

or

$$\sum_i x_i(G_i^{\infty,\,\text{aq}} + \Delta G_i) = \sum_i x_i[G_i^{\infty,\,\text{aq}} + RT\ln \gamma_i^{*}(x_m \to 0)],\quad i = c,\ a \tag{43}$$

$$\sum_i x_i(H_i^{\infty,\,\text{aq}} + \Delta H_i) = \sum_i x_i\left[H_i^{\infty,\,\text{aq}} - RT^2\frac{\partial \ln \gamma_i^{*}(x_m \to 0)}{\partial T}\right],\quad i = c,\ a \tag{44}$$

Therefore, the Gibbs free energy and enthalpy corrections ΔG_i and ΔH_i can be calculated, respectively, by the following equations:

$$\Delta G_i = RT\ln \gamma_i^{*}(x_m \to 0),\quad i = c,\ a \tag{45}$$

$$\Delta H_i = -RT^2\frac{\partial \ln \gamma_i^{*}(x_m \to 0)}{\partial T},\quad i = c,\ a \tag{46}$$

or

$$G_i^{\text{fused}} = G_i^{\infty,\,\text{aq}} + RT\ln \gamma_i^{*}(x_m \to 0),\quad i = c,\ a \tag{47}$$

$$H_i^{\text{fused}} = H_i^{\infty,\,\text{aq}} - RT^2\frac{\partial \ln \gamma_i^{*}(x_m \to 0)}{\partial T},\quad i = c,\ a \tag{48}$$

Given liquid enthalpy, we can proceed to calculate heat of mixing, heat of dilution, and heat of solution. They are calorimetric

Table 1. Summary of Model Parameters

parameters	component	source	data for regression
Antoine equation parameters	H_2SO_4	Regression	VLE for $H_2SO_4-H_2O-SO_3$
	SO_3	Aspen Plus Databank[13]	
	$H_2S_2O_7$	Nonvolatile	
$\Delta_f H^{ig}_{m,298.15}$	H_2O, H_2SO_4, SO_3	Aspen Plus Databank[13]	
$C^{ig}_{p,m}$	H_2O, H_2SO_4, SO_3	Aspen Plus Databank[13]	
$\Delta_f H^{liq}_{m,298.15}$	$H_2S_2O_7$	Regression	heat of solution for $SO_3-H_2SO_4$
$C^{liq}_{p,m}$	$H_2S_2O_7$	Regression	heat of solution for $SO_3-H_2SO_4$
$\Delta_{vap}H_m$	H_2O, H_2SO_4, SO_3	Aspen Plus Databank[13]	
$\Delta_f H^{\infty,aq}_{i,298.15}$	H_3O^+,	Aspen Plus Databank[13]	
	HSO_4^-, SO_4^{-2}	Wagman et al.[14]	
	$H_5O_2^+$	Regression	Heat of dilution for $H_2SO_4-H_2O$
$C^{\infty,aq}_{p,i}$	H_3O^+	Aspen Plus Databank[13]	
	HSO_4^-, SO_4^{-2}	Wagman et al.[14]	
	$H_5O_2^+$	Regression	Heat capacity for $H_2SO_4-H_2O$
eNRTL binary parameters	molecule−molecule binary	Regression	VLE, heat of dilution, heat capacity, speciation and osmotic coefficient for $H_2SO_4-H_2O-SO_3$
	molecule−electrolyte binary	Regression	VLE, heat of dilution, heat capacity, speciation and osmotic coefficient for $H_2SO_4-H_2O-SO_3$
	electrolyte−electrolyte binary	Regression	VLE, heat of dilution, heat capacity, speciation and osmotic coefficient for $H_2SO_4-H_2O-SO_3$
dielectric constant equation parameters	H_2O, H_2SO_4	Aspen Plus Databank[13]	
	SO_3	Maryott and Smith[15]	
	$H_2S_2O_7$	assumed the same as H_2SO_4	
A_i, B_i, for ln K_i	R_1 to R_5	Regression	VLE, heat of dilution, heat capacity, speciation and osmotic coefficient for $H_2SO_4-H_2O-SO_3$

quantities often reported in the literature. Heat of dilution is the heat effect per unit mole of solute for a dilution process in which solvent is added to a solution to dilute the solute. Heat of solution is the heat effect per unit mole of solute for a solution process in which solute is added to a solution. Both heat of dilution and heat of solution can be calculated through enthalpy balance, as described by the following equation:

$$\Delta H = \frac{h_{final} - h_{initial} - h_{add}}{n_{solute}} \quad (49)$$

where, ΔH is heat of dilution or heat of solution, h_{final} is the enthalpy of the final solution; $h_{initial}$ is the enthalpy of the initial solution; h_{add} is the enthalpy of the solvent or solute added to the initial solution to form the final solution, n_{solute} is the number of moles of solute in the initial solution for the dilution process and the number of moles of solute added to the solution for the solution process.

MODEL PARAMETERS

Table 1 summarizes the model parameters associated with the thermodynamic framework. The model parameters include pure component parameters and thermodynamic constants for the molecular and ionic species, the binary interaction parameters associated with the symmetric electrolyte NRTL model, and the chemical equilibrium constants for the liquid phase reactions.

The Antoine equation is given as follows:

$$\ln p_i = C_{1i} + \frac{C_{2i}}{T + C_{3i}} + C_{4i}T + C_{5i}\ln T + C_{6i}T^{C_{7i}} \quad (50)$$

where p_i is vapor pressure in Pa of component i, T is the temperature in K, and C_{1i}, C_{2i}, ..., C_{7i} are Antoine equation parameters for component i. The Antoine equation parameters for pure component vapor pressure are taken from DIPPR[13] for sulfur trioxide, as summarized in Table 2. The Antoine equation parameters for sulfuric acid are adjusted to correlate the data on partial pressure of sulfuric acid. Disulfuric acid is treated as nonvolatile.

The ideal gas Gibbs free energy and enthalpy of molecular species m are calculated, respectively, from the following expressions:

$$G^{ig}_m = \Delta_f H^{ig}_{m,298.15} - \left(\frac{T}{298.15}\right)(\Delta_f H^{ig}_{m,298.15} - \Delta_f G^{ig}_{m,298.15}) + \int_{298.15}^{T} C^{ig}_{p,m}\,dT - T\int_{298.15}^{T}\frac{C^{ig}_{p,m}}{T}\,dT \quad (51)$$

$$H^{ig}_m = \Delta_f H^{ig}_{m,298.15} + \int_{298.15}^{T} C^{ig}_{p,m}\,dT \quad (52)$$

where $\Delta_f G^{ig}_{m,298.15}$ and $\Delta_f H^{ig}_{m,298.15}$ are the ideal gas Gibbs free energy and enthalpy of formation of molecular species m at 298.15 K, respectively, and $C^{ig}_{p,m}$ is the ideal gas heat capacity of molecular species m calculated from the DIPPR correlation:

$$C^{ig}_{p,m} = A_m + B_m\left(\frac{C_m/T}{\sinh(C_m/T)}\right)^2 + D_m\left(\frac{E_m/T}{\cosh(E_m/T)}\right)^2 \quad (53)$$

where A_m, B_m, C_m, D_m, and E_m are the correlation parameters.

Watson's equation[13] for the heat of vaporization is expressed as follows:

$$\Delta_{vap}H_m(T) = \Delta_{vap}H_m(T_1)\left(\frac{1 - T/T_{C,m}}{1 - T_1/T_{C,m}}\right)^{a_m + b_m(1 - T/T_{C,m})} \quad (54)$$

dx.doi.org/10.1021/je100930y |J. Chem. Eng. Data 2011, 56, 963–977

Table 2. Antoine Equation Parameters

components	SO_3	H_2SO_4
source	Aspen Plus Databank[13]	this work
C_1	180.99	36.725
C_2	−12060.0	−9544.7
C_3	0.0	0.0
C_4	0.0	0.00022
C_5	−22.839	−1.8261
C_6	7.235×10^{-17}	0.0
C_7	6.0	2.0

where $\Delta_{vap}H_m(T)$ is the heat of vaporization of component m at temperature T, $\Delta_{vap}H_m(T_1)$ is the heat of vaporization of component m at a reference temperature T_1, T and T_1 are temperatures in K, $T_{C,m}$ is the critical temperature of component m, and a_m and b_m are component-specific correlation parameters.

The liquid enthalpy of nonvolatile disulfuric acid is calculated from the enthalpy of formation of liquid $H_2S_2O_7$ at 298.15 K and 101325 Pa and the heat capacity of liquid $H_2S_2O_7$

$$H_m^l = \Delta_f H_{m,298.15}^{liq} + \int_{298.15}^{T} C_{p,m}^{liq}\, dT \qquad (55)$$

where $\Delta_f H_{m,298.15}^{liq}$ is the enthalpy of formation of liquid molecular species m at 298.15 K and $C_{p,m}^{liq}$ is the liquid heat capacity of molecular species m.

Tables 3−5 list pure component property parameters required for enthalpy calculations. These parameters include the following: (1) for sulfuric acid, water and sulfur trioxide, ideal gas enthalpy of formation at 298.15 K, ideal gas heat capacity correlation parameters, and Watson heat of vaporization correlation parameters, (2) for disulfuric acid, liquid enthalpy of formation at 298.15 K and liquid heat capacity, and (3) for ionic species, aqueous phase infinite dilution enthalpy of formation and aqueous phase infinite dilution heat capacity correlation parameters. While these parameters are mainly retrieved from Aspen Plus databanks[13] or the NBS Tables of Wagman et al.,[14] the aqueous phase infinite dilution enthalpy of formation and heat capacity for $H_5O_2^+$ are identified by regression against heat of dilution data and heat capacity data of the aqueous sulfuric acid solution.

For disulfuric acid, the liquid enthalpy of formation and heat capacity are identified by regression against the heat of solution data for liquid SO_3 in H_2SO_4. We further assume the aqueous phase infinite dilution heat capacity of the ions to be temperature-independent in this work.

The Redlich−Kwong equation-of-state model parameters taken from the Aspen Plus databank[13] are summarized in Table 6.

eNRTL binary interaction parameters are required to describe the short-range interactions in the electrolyte NRTL activity coefficient model. There can be molecule−molecule binary parameters, molecule−electrolyte binary parameters, and electrolyte−electrolyte binary parameters. Following the convention of the eNRTL model,[7] we set the default values to 0 for molecule−molecule parameters and electrolyte−electrolyte parameters, 8 for molecule−electrolyte parameters, and −4 for electrolyte−molecule parameters. These values represent typical values for these binary parameters. The eNRTL binary parameters for the water−(H_3O^+, HSO_4^-) binary, water−($H_5O_2^+$, HSO_4^-) binary, water−(H_3O^+, SO_4^{-2}) binary, water−($H_5O_2^+$, SO_4^{-2}) binary, sulfuric acid−(H_3O^+, HSO_4^-) binary, ($H_5O_2^+$, HSO_4^-)−($H_5O_2^+$, SO_4^{-2}) binary, and (H_3O^+, HSO_4^-)−($H_5O_2^+$, HSO_4^-) binary are treated as adjustable model parameters and regressed from the available experimental data. The eNRTL parameters for the water-sulfuric acid pair are not adjusted because water and sulfuric acid do not become dominant species in the system at the same time. On the other hand, the eNRTL parameters for the sulfuric acid−sulfur trioxide pair are treated as adjustable parameters. For the nonrandomness factor, 0.3 is used for all molecule−molecule pairs and 0.2 for all molecule−electrolyte pairs and electrolyte−electrolyte pairs. Experimental data of VLE, speciation, osmotic coefficient, heat of mixing and heat of dilution, and heat capacity are then used to identify the eNRTL binary interaction parameters.

Table 3. Pure Component Property Parameters for Enthalpy

components	$\Delta_f H_{m,298.15}^{ig}$ / kJ·mol^{-1}	$\Delta_f H_{i,298.15}^{\infty,aq}$ / kJ·mol^{-1}	$C_{p,i}^{\infty,aq}$ / J·mol^{-1}·K^{-1}	$\Delta_f H_{m,298.15}^{liq}$ / kJ·mol^{-1}	$C_{p,i}^{liq}$ / J·mol^{-1}·K^{-1}
H_2O	−241.81[a]				
H_2SO_4	−735.20[a]				
SO_3	−395.72[a]				
$H_2S_2O_7$				−1275.0[b]	26.934[b]
H_3O^+		−285.83[a]	75.291[a]		
$H_5O_2^+$		−574.87[b]	466.70[b]		
HSO_4^-		−887.34[c]	−84.0[c]		
SO_4^{-2}		−909.27[c]	−293.0[c]		

[a] Parameters taken from Aspen Plus databank[13] [b] Parameters regressed. [c] Parameters taken from Wagman et al.[14]

Table 4. DIPPR Ideal Gas Heat Capacity Model Parameters from Aspen Plus Databank[13]

parameter	H_2O	H_2SO_4	SO_3
A/J·kmol^{-1}·K^{-1}	33363	40240	33408
B/J·kmol^{-1}·K^{-1}	26790	109500	49677
C/K	2610.5	943	873.22
D/J·mol^{-1}·K^{-1}	8896	83700	28563
E/K	1169	393.8	393.74

Table 5. Watson Heat of Vaporization Model Parameters from Aspen Plus Databank[13]

parameter	H_2O	H_2SO_4	SO_3
$\Delta_{vap}H_m(T_1)$/ kJ·mol^{-1}	40.683	85.0	40.679
T_1/K	373.20	298.15	318.00
a_m	0.3106	0.38	0.3633
b_m	0.0	0.0	0.0

Dielectric constants of molecular solvents are required by the electrolyte NRTL model in the calculation of the long-range interactions. Table 7 summarizes the dielectric constant correlation parameters in eq 14 and their sources. Unlike water, dielectric constant data of sulfuric acid and sulfur trioxide[15] are rare and they are treated as constants. The dielectric constant of disulfuric acid is assumed to be the same as that of sulfuric acid.

The equilibrium constants can be related to the molar liquid Gibbs free energies of molecular species at the system temperature and pressure and of ionic species at the pure fused salt state as follows:

$$\ln K_i = -\frac{\Delta G_i}{RT} \qquad (56)$$

where ΔG_i is the Gibbs free energy change of reaction R_i.

dx.doi.org/10.1021/je100930y |J. Chem. Eng. Data 2011, 56, 963–977

Table 6. Redlich−Kwong Equation of State Model Parameters

components	H_2O	H_2SO_4	SO_3
source	Aspen Plus Databank[13]	Aspen Plus Databank[13]	Aspen Plus Databank[13]
T_c/K	647.096	925	490.85
P_c/MPa	22.064	6.400	8.210

In this work, the equilibrium constants of the reactions R1 to R5 are treated as adjustable parameters with the following empirical correlation:

$$\ln K_i = A_i + \frac{B_i}{T} \quad (57)$$

where K_i is the chemical equilibrium constant for reaction R_i and A_i and B_i are correlation parameters for reaction R_i. A_i and B_i for the reactions are identified through regression. The regressed equilibrium constants are checked to ensure consistency with Gibbs free energy calculations.

EXPERIMENTAL DATA AND DATA TREATMENT

Due to the critical importance of the sulfuric acid system, numerous experimental data sets are available in the literature. With the aim to develop a comprehensive thermodynamic model for the sulfuric acid system, we focus on the major compilations of literature data for VLE,[12,16−22] speciation,[23−29] osmotic coefficient,[30,31] heat of dilution,[14,32,33] heat of mixing,[32,33] heat of solution,[34] and liquid heat capacity[35] of the sulfuric acid system.

Vapor−Liquid Equilibrium Data. Gmitro and Vermeulen[16] estimated total pressures and partial pressures of sulfuric acid, water and sulfur trioxide over the aqueous sulfuric acid solutions based on liquid phase pure and partial molal thermodynamic quantities and vapor phase pure component thermodynamic properties from (223 to 673) K for sulfuric acid compositions from 0.10 mass fraction to unity mass fraction. These total pressure and partial pressure data are plotted in Figures 2 to 5 together with measured or estimated data from other sources.[12,19−21] The estimation results of Gmitro and Vermeulen for concentrated sulfuric acid solutions especially at low temperatures were later challenged[17,18] and revised.[19]

Roedel[17] measured sulfuric acid partial pressure over two concentrated aqueous sulfuric acid solutions at 296.15 K and found the measurements to be only about one tenth of the estimates of Gmitro and Vermeulen. Roedel concluded that the estimated data of Gmitro and Vermelen, although widely used, might be too large in sulfuric acid partial pressure at room temperature.

Sulfuric acid partial pressure of 0.9801 mass fraction aqueous sulfuric acid solution at temperatures from 333 to 453 K were measured by Ayers et al.[18] Again, their reported vapor pressures are about 1 order of magnitude smaller than those estimated by Gmitro and Vermeulen. They also extrapolated their measured results to the condition investigated by Roedel and the extrapolation yielded generally consistent sulfuric acid partial pressures with the results of Roedel.

On the basis of the results of Ayers et al., Vermeulen et al.[19] presented recalculated partial pressures of sulfuric acid, water and sulfur trioxide at the conditions similar to those of Gmitro and Vermeulen, i.e., at temperatures from (273 to 623) K and sulfuric acid concentrations from 0.10 mass fraction to unity mass fraction. The updated total pressures are consistent with the Gmitro and Vermeulen results up to about 0.98 mass fraction sulfuric acid (~ 0.47 mol fraction SO_3), but much lower than the Gmitro and Vermeulen results when the acid concentration is further increased, as shown in Figure 2b. Above 0.98 mass fraction sulfuric acid, the total pressures are dominated initially by the sulfuric acid partial pressures and then by the SO_3 partial pressures. The study by Vermeulen et al. yielded 1 order of magnitude lower sulfuric acid partial pressures at the high acid concentration region. See Figure 3. Water partial pressures and SO_3 partial pressures in this region are generally consistent between these two studies, as shown in Figures 4 and 5. These two studies do show extremely different water and SO_3 partial pressures when approaching pure sulfuric acid, i.e, SO_3 mole fraction approaching 0.5. At this near pure acid concentration, the Vermeulen et al. study estimated higher water partial pressures and lower SO_3 partial pressures than the study by Gmitro and Vermeulen.

Table 7. Dielectric Constant Parameters

components	H_2O	H_2SO_4	SO_3	$H_2S_2O_7$
source	Aspen Plus Databank[13]	Aspen Plus Databank[13]	Maryott and Smith[15]	this work
A	78.51	101	3.11	101[a]
B	31989.4	0	0	0[a]
C	298.15	298.15	291.15	298.15[a]

[a] Parameters for $H_2S_2O_7$ are assumed the same as those of H_2SO_4 in Aspen Plus Databanks.[13]

Wüster[20] reported experimental measurements of total pressures of aqueous sulfuric acid solutions with concentrations from 0.70 to 0.996 mass fraction at elevated temperatures from 413 to 753 K. This elevated temperature data shows reasonable agreement with the Gmitro and Vermeulen data up to 0.985 mass fraction although slightly higher for more concentrated solutions. Figure 6 shows a total pressure−temperature plot for a 0.985 mass fraction sulfuric acid solution. The Wüster data for 0.9861 mass fraction solution cover temperature from (549 to 754) K and they seem consistent with the data of Gmitro and Vermeulen for 0.985 mass fraction solution which are slightly higher than those of Vermeulen et al.

Bolsaitis and Elliott[21] reviewed data of thermodynamic activities and vapor pressures of aqueous sulfuric acid solutions and presented their pressure calculations from (273 to 603) K for aqueous sulfuric acid solution up to the azeotropic concentrations, around 0.984 to 0.988 mass fraction. The methodology was similar to that used by Gmitro and Vermeulen and Vermeulen et al. However, Bolsaitis and Elliott made use of a different thermodynamic property database, especially with new measurements such as those of Roedel[17] and Wüster.[20] The resulting total pressures are close to those of Vermeulen et al. at temperatures up to 473 K, as shown in Figure 2c. The same behavior is also observed for sulfuric acid partial pressure, as shown by Figure 3. For water partial pressure, the Bolsaitis and Elliott results are in line with those of the Gmitro and Vermeulen study and the study by Vermeulen et al. at concentrations up to 0.98 mass fraction sulfuric acid concentrations but lower than these two for more concentrated solutions at temperatures lower than 473 K, as shown by Figure 4. Figure 4 also shows the Bolsaitis and Elliott study yielded some unusually high water partial pressure results at high acid concentrations, i.e., SO_3 mole fraction around 0.4,

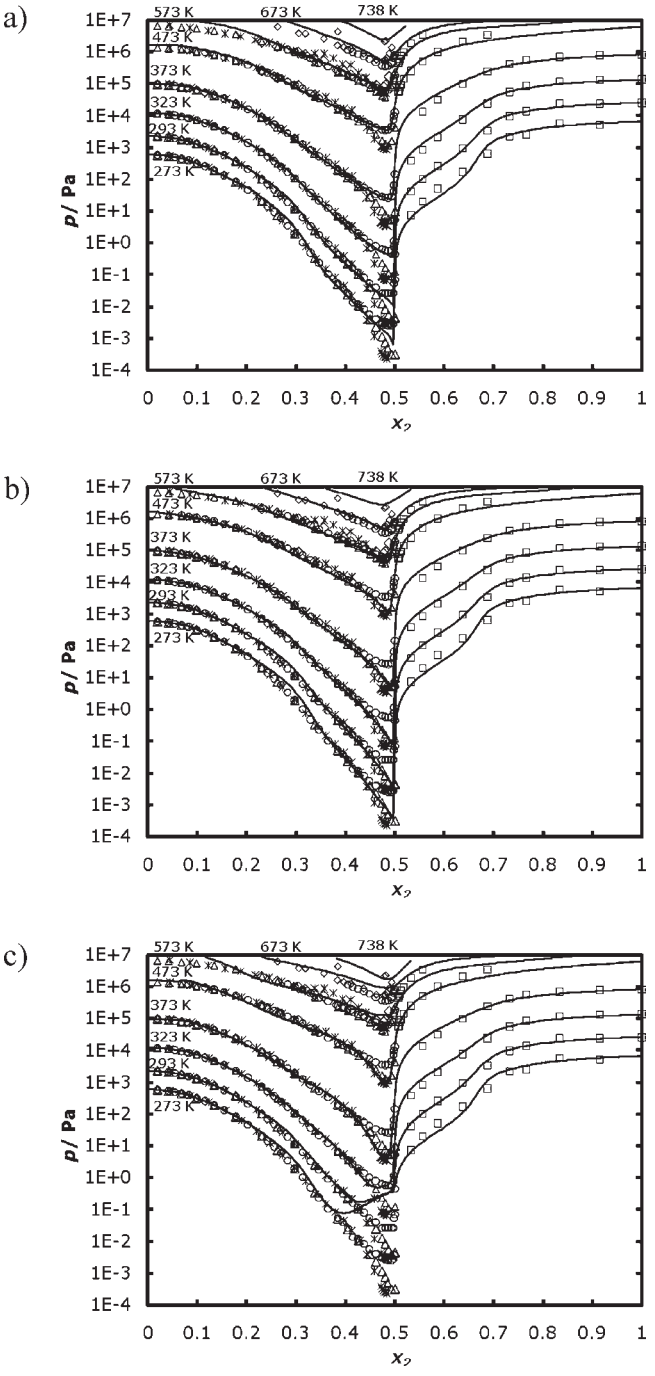

Figure 2. a. Total pressure p of the sulfuric acid system, water (1) + sulfur trioxide (2), versus mole fraction of apparent sulfur trioxide x_2. ○, ref 16; Δ, ref 19; *, ref 21; □, ref 20; ×, ref 12; —, model results with model parameters regressed from estimated VLE data of ref 16. b. Total pressure p of the sulfuric acid system, water (1) + sulfur trioxide (2), versus mole fraction of apparent sulfur trioxide x_2. ○, ref 16; Δ, ref 19; *, ref 21; ◇, ref 20; ×, ref 12; —, model results with model parameters regressed from estimated VLE data of ref 19. c. Total pressure p of the sulfuric acid system, water (1) + sulfur trioxide (2), versus mole fraction of apparent sulfur trioxide x_2. ○, ref 16; Δ, ref 19; *, ref 21; □, ref 20; ×, ref 12; —, model results with model parameters regressed from estimated VLE data of ref 21.

and high temperatures, i.e., 573 K. These unusually high water partial pressures resulted in a major jump for the total pressure at SO_3 mole fraction around 0.4 and 573 K. See Figure 7.

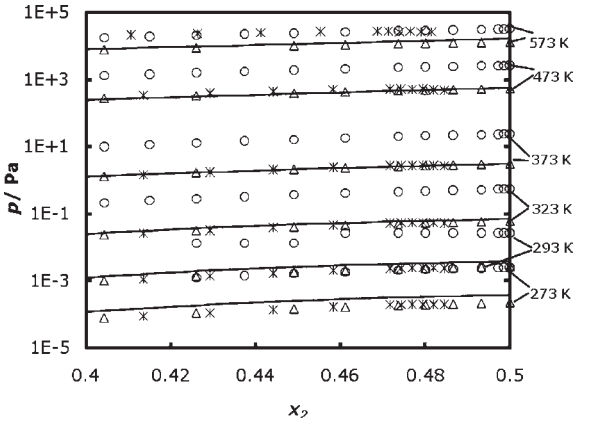

Figure 3. Partial pressure of sulfuric acid p of the sulfuric acid system, water (1) + sulfur trioxide (2), versus mole fraction of apparent sulfur trioxide x_2 . ○, ref 16; Δ, ref 19; *, ref 21; —, model results with model parameters regressed from estimated VLE data of ref 19.

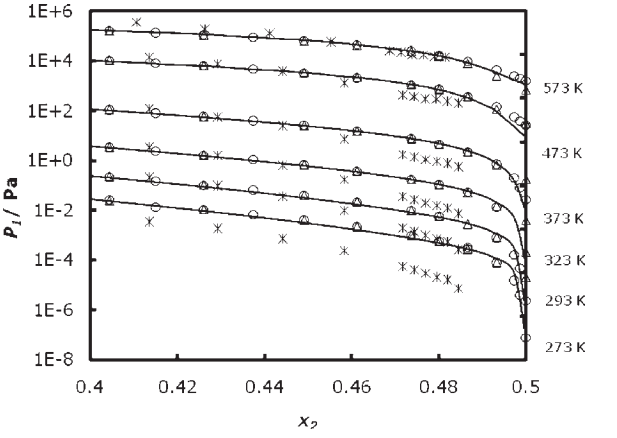

Figure 4. Partial pressure of water p_1 of the sulfuric acid system, water (1) + sulfur trioxide (2), versus mole fraction of apparent sulfur trioxide x_2. ○, ref 16; Δ, ref 19; *, ref 21; —, model results with model parameters regressed from estimated VLE data of ref 19.

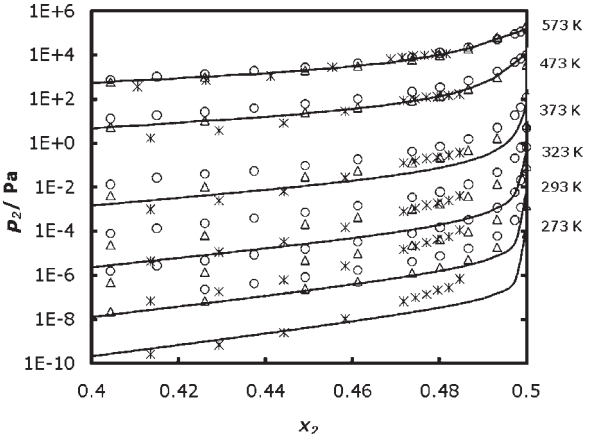

Figure 5. Partial pressure of sulfur trioxide p_2 of the sulfuric acid system, water (1) + sulfur trioxide (2),versus mole fraction of apparent sulfur trioxide x_2. ○, ref 16; Δ, ref 19; *, ref 21; —, model results with model parameters regressed from estimated VLE data of ref 19.

dx.doi.org/10.1021/je100930y |J. Chem. Eng. Data 2011, 56, 963–977

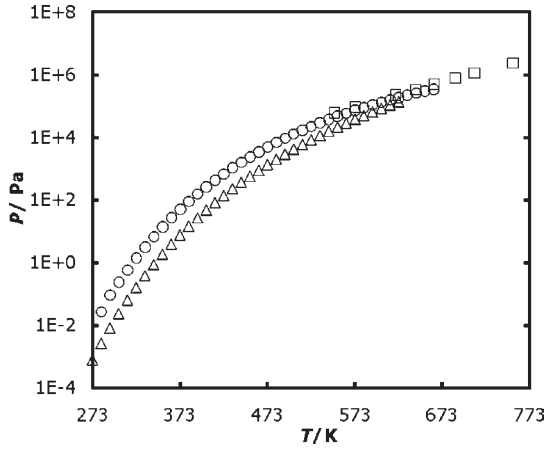

Figure 6. Total pressure p of aqueous sulfuric acid system, water (1) + sulfuric acid (2), at mass fraction of apparent sulfuric acid w_2 = 0.985, versus temperature T. ○, ref 16; Δ, ref 19; □, ref 20.

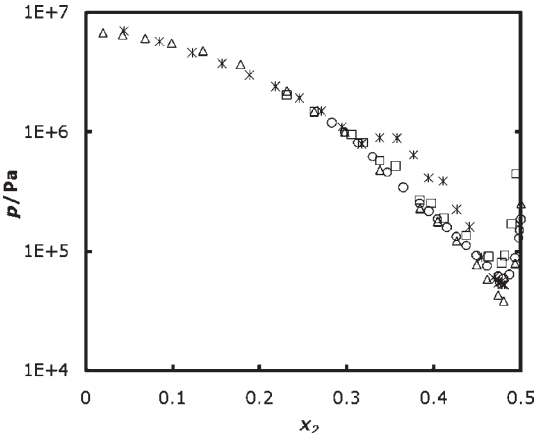

Figure 7. Total pressure p of the sulfuric acid system, water (1) + sulfur trioxide (2) at T = 573.15 K, versus mole fraction of apparent sulfur trioxide x_2. ○, ref 16; Δ, ref 19; *, ref 21; □, ref 20.

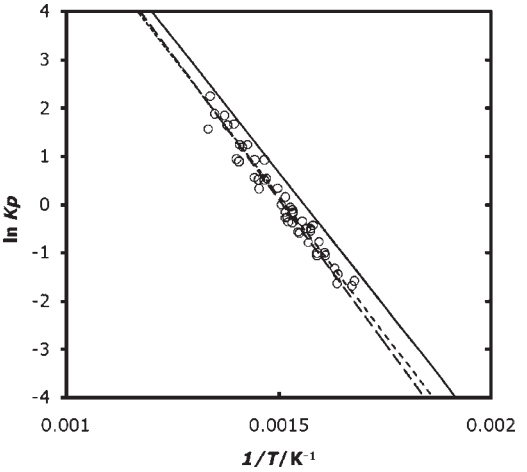

Figure 8. Natural logarithm of the equilibrium constant of the sulfuric acid decomposition reaction ln Kp versus reciprocal of temperature $1/T$. ○, ref 36; ---, calculated from ref 16; —, calculated from ref 19; — — —, calculated from ref 21.

These three studies derived partial pressures of SO_3 from partial pressures of water, sulfuric acid, and the chemical equilibrium constant of the sulfuric acid decomposition reaction in the vapor phase. Although they all cited the chemical equilibrium constant data of Bodenstein and Katayama,[16,36] it is found that the Gmitro and Vermeulen results and the Bolsaitis and Elliott results could match the Bodenstein and Katayama[36] study better than the Vermeulen et al. results could in the temperature range covered by the study of Bodenstein and Katayama. Figure 8 shows the Vermeulen et al. results gave slightly higher chemical equilibrium constants. For this reason and the disagreements in partial pressures of water and sulfuric acid, the partial pressures for SO_3 are quite different among the three studies, especially at low concentrations and low temperatures. Better consistency is observed at high temperatures and high concentrations, as shown by Figure 5.

In summary, there are three major estimation studies on VLE of aqueous sulfuric acid solutions, those of Gmitro and Vermeulen, Vermeulen et al., and Bolsaitis and Elliott. These three studies generally agree with each other at low concentrations but yield significantly different results for concentrated aqueous sulfuric acid solutions. The experimental studies of Roedel[17] and Ayers et al.[18] on sulfuric acid partial pressure of concentrated sulfuric acid solutions at room temperature suggest those of Gmitro and Vermeulen are too high and they support estimations of Vermeulen et al. and Bolsaitis and Elliott at low temperatures. However, the experimental study of Wüster[20] on total pressures of aqueous sulfuric acid systems from 0.70 to 0.996 mass fraction at elevated temperatures shows reasonable agreement with the data of Gmitro and Vermeulen and, to a lesser extent, the data of Vermeulen et al. In this study, we attempted to use these three sets of data in the regression. Our results will be discussed in later sections.

In addition to the VLE data shown above for the aqueous sulfuric acid system, Kunzler[22] reported useful azeotropic concentration data at pressures from 13 to 130 kPa. These azeotrope data provide an additional validation check for the model.

For the VLE data of the oleum system, i.e., from unity mass fraction sulfuric acid to unity mass fraction sulfur trioxide, we use the experimental study of Schrage.[12]

Speciation Data. Speciation of sulfuric acid in aqueous solution has been extensively studied[23−29] mostly by spectroscopy measurements of the aqueous sulfuric acid solutions. The various studies revealed that (1) the first dissociation of sulfuric acid is complete in diluted solutions but partial in concentrated solutions, (2) the second dissociation of sulfuric acid is also partial dissociation, (3) extents of both first and second dissociations of sulfuric acid decrease with increase of temperature, and (4) hydrated proton ions exist in the aqueous sulfuric acid solutions, especially for dilute solutions.

The available experimental measurements on the degree of dissociation of the bisulfate ion, $\eta_{HSO_4^-}$, at 298.15 K from several different sources[23−29] are plotted in Figure 9. While significant discrepancies exist among data from different sources, the data from Lindstrom et al.[23] and the data from Young et al.[24] seem to be representative of the speciation data. We choose to use these two speciation data sets in regression. In addition, some of data of Sherrill and Noyes[25] is also used to supplement data at the very dilute region.

Osmotic Coefficient Data. Rard et al.[30] reviewed and updated osmotic coefficient data for aqueous sulfuric acid solutions at 298.15 K with acid concentration from (1 to 27) m. In addition

dx.doi.org/10.1021/je100930y |J. Chem. Eng. Data 2011, 56, 963–977

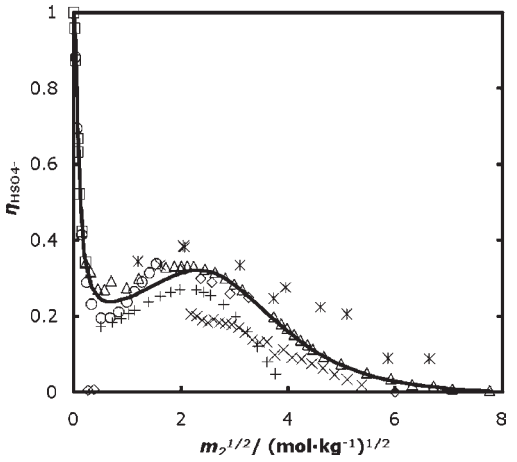

Figure 9. Degree of dissociation of bisulfate ion $\eta_{HSO_4^-}$ in water (1) + sulfuric acid (2) solutions at T = 298.15 K, versus the square root of molality of apparent sulfuric acid $m_2^{1/2}$. ○, ref 23; Δ, ref 24; □, ref 25; +, ref 26; × , ref 27; ◇, ref 28; *, ref 29; —, model results.

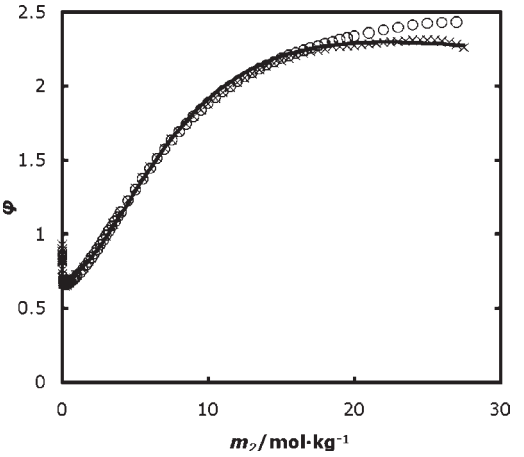

Figure 10. Osmotic coefficients φ of aqueous sulfuric acid system, water (1) + sulfuric acid (2), at T = 298.15 K, versus molality of apparent sulfuric acid m_2. ○, ref 30; × , ref 31; —, model results.

to the osmotic coefficient data, they also reported the corresponding values for water activity and mean ionic activity coefficient.

Another extensive review and compilation of osmotic coefficient data and water activity data at room temperature was reported by Staples[31] for aqueous sulfuric acid solutions with acid concentration from (0.001 to 27.5) m.

Figure 10 shows the osmotic coefficient data of Rard et al.[30] and the data of Staples[31] agree with each other up to 15 m. Starting from 15 m, the values of Rard et al. become slightly greater than those of Staples. Both of these data sets are used in data regression. We should note that these osmotic coefficient data are converted to apparent water activity coefficients for the purpose of data regression.

Enthalpy and Heat Capacity Data. The NBS tables of chemical thermodynamic properties compiled by Wagman et al.[14] provide an extensive set of data for molar heat of formation of sulfuric acid diluted in various moles of water at 298.15 K. From such data we obtain values for molar heat of dilution of sulfuric acid with water.

Rütten et al.[32] and Kim and Roth[33] measured heat of dilution for aqueous sulfuric acid systems at 283 K, 293 K, 313 K, and 333 K. They also derived heat of mixing from the heat of dilution data. Their studies revealed that the heat of dilution of the H_2SO_4−H_2O binary system does not depend on temperature. Comparison between the NBS data at 298.15 K and the Kim and Roth data at 283 K, 293 K, 313 K, and 333 K supports this conclusion. See Figure 11. Data from these two sources at different temperatures agree with each other very well. In this work, the NBS data are used in the regression to identify necessary parameters in the enthalpy model, i.e., infinite dilution enthalpy of formation of the $H_5O_2^+$ ion. Then, the data from Rütten et al. and Kim and Roth are used for validation of the model.

Calorimetric effects of the SO_3−H_2SO_4 binary system and reported heat of solution of liquid SO_3 in oleum systems at 303.15 K was studied by Miles et al.[34] This data is used in regression to identify the enthalpy of formation and heat capacity of disulfuric acid.

Heat capacity data for the aqueous sulfuric acid solution at 293.15 K have been reported in Perry's Handbook.[35] The data cover the sulfuric acid concentration from pure water to pure sulfuric acid and they are used in regression to identify the

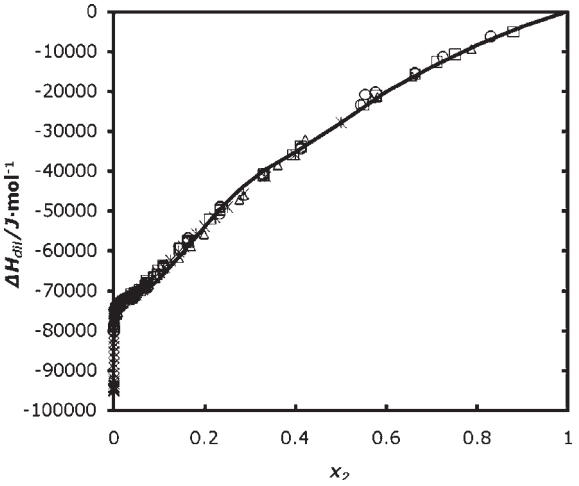

Figure 11. Heat of dilution ΔH_{dil} of aqueous sulfuric acid system, water (1) + sulfuric acid (2), versus mole fraction of apparent sulfuric acid x_2. ○, ref 33 at T = 293.15 K; □, ref 33 at T = 313.15 K; Δ, ref 33 at T = 333.15 K; *, ref 14 at T = 298.15 K; —, model results at T = 298.15 K.

parameters in the enthalpy model, i.e., the aqueous phase infinite dilution heat capacity for the $H_5O_2^+$ ion.

DATA REGRESSION

We conduct simultaneous regression of all of the thermophysical property data summarized in Table 8: VLE data[12,16,19,21] for the sulfuric acid system from (273 to 573) K, speciation or degree of dissociation data[23−25] of the bisulfate ion at 298.15 K, osmotic coefficient data[30,31] at 298.15 K, heat of dilution data[14] of sulfuric acid in water at 298.15 K, heat of solution data[34] for liquid SO_3 in oleum systems at 303.15 K, and heat capacity data[35] of the aqueous sulfuric acid solution at 293.15 K. The adjustable parameters include the following:

- Antoine equation parameters for sulfuric acid
- liquid enthalpy of formation and liquid heat capacity of disulfuric acid
- aqueous phase infinite dilution enthalpy of formation and heat capacity for $H_5O_2^+$ ion

Table 8. Experimental Data Used in Regression

source	data type	system	T, K	concentration	n^b	ARD,[d] %
Gmitro and Vermeulen[16]	P_{H2O}, P_{H2SO4}, and P_{SO3}	H_2SO_4/H_2O	273−573	0.10−1.00 mass frac H_2SO_4	255[c]	29.38
Vermeulen et al.[19]	P_{H2O}, P_{H2SO4}, and P_{SO3}	H_2SO_4/H_2O	273−573	0.10−1.00 mass frac H_2SO_4	151	23.73
Bolsaitis and Elliott[21]	P_{H2O}, P_{H2SO4}, and P_{SO3}	H_2SO_4/H_2O	273−573	0∼azeotropic points	195[c]	39.85
Schrage[12]	P_{SO3}	H_2SO_4/SO_3	273−573	0.02−1.00 mol frac free SO_3[a]	53	23.54
Lindstrom and Wirth[23]	Speciation	H_2SO_4/H_2O	298	0−2.5 m H_2SO_4	9	10.95
Young et al.[24]	Speciation	H_2SO_4/H_2O	298	2.5−60 m H_2SO_4	24	4.20
Sherrill and Noyes[25]	Speciation	H_2SO_4/H_2O	298	0−0.025 m H_2SO_4	5	8.81
Rard et al.[30]	Osmotic coefficients	H_2SO_4/H_2O	298	1−27 m H_2SO_4	64	1.85
Staples[31]	Osmotic coefficients	H_2SO_4/H_2O	298	0.001−27.5 m H_2SO_4	81	1.44
Wagman et al.[14]	Heat of dilution	H_2SO_4/H_2O	298	0−0.5 mol frac H_2SO_4	55	1.12
Miles et al.[34]	Heat of solution	H_2SO_4/SO_3	303	0.01−0.80 mass frac free SO_3[a]	13	5.34
Perry's Handbook[35]	Heat capacity	H_2SO_4/H_2O	293	0−1.00 mass frac H_2SO_4	38	1.35

[a] Free SO_3 refers to apparent SO_3 in a $H_2SO_4-SO_3$ binary system. [b] n is number of data points in a data set. [c] Excluded from regression for the final model. [d] ARD is average relative deviation of the calculated results of the final model from the experimental data, and defined as $(\sum_n(|EST - EXP|)/(EXP)/n) \times 100\%$, where n is number of data points, EST is calculated results of the final model, and EXP is experimental data.

•eNRTL binary interaction parameters for the $SO_3-H_2SO_4$ binary, the $H_2O-(H_3O^+, HSO_4^-)$ binary, the $H_2O-(H_5O_2^+, HSO_4^-)$ binary, the $H_2O-(H_3O^+, SO_4^{-2})$ binary, the $H_2O-(H_5O_2^+, SO_4^{-2})$ binary, the $H_2SO_4-(H_3O^+, HSO_4^-)$ binary, the $(H_5O_2^+, HSO_4^-)-(H_5O_2^+, SO_4^{-2})$ binary, and the $(H_3O^+, HSO_4^-)-(H_5O_2^+, HSO_4^-)$ binary.

•chemical equilibrium constant parameters for reactions R1 to R5

Standard deviations of the experimental data used in the regression are assigned according to the following rules:

•0.1 K for temperatures

•10% for pressures

•0.001 for mass fraction or mole fraction compositions

•0.1% for water activity coefficient (computed from osmotic coefficient)

•5% for degree of bisulfate dissociation

•1% for heat of dilution of aqueous sulfuric acid systems and heat of solution data for oleum system

•0.5% for heat capacity of aqueous sulfuric acid solutions

The regression runs are executed to minimize the residue root-mean-square error (RRMSE) defined as:

$$\mathrm{RRMSE} = \sqrt{\frac{\sum_{i=1}^{k}\sum_{j=1}^{m}\left(\frac{Z_{ij} - ZM_{ij}}{\sigma_{ij}}\right)^2}{k - n}} \qquad (58)$$

where ZM = measured (experimental) value, Z = calculated value, σ = standard deviation, i = data point number, k = total number of data points, j = measured variable for a data point (such as temperature, pressure, or mole fraction), m = number of measured variables for a data point, n = total number of adjustable parameters.

RESULTS AND DISCUSSION

Due to the inconsistencies that exist among the three major VLE data sets for aqueous sulfuric aicd solutions, we perform three separate data regression runs, each with one of the three VLE data sets of aqueous sulfuric acid solutions included in regression: (1) VLE data from Gmitro and Vermeulen, (2) VLE data from Vermeulen et al., and (3) VLE data from Bolsaitis and Elliott. All other data in Table 8 is also included in the three regression runs. To avoid excessive weight on potentially questionable data, we remove from the regression runs those VLE data points with pressure lower than 1 Pa. Many of the removed data points are sulfuric acid partial pressures and sulfur trioxide partial pressures for concentrated acid solutions at low temperatures, i.e., below 373 K.

The regressions yield the residue root-mean-square error (RRMSE) of 1.995 and 1.987 for the run with the VLE data of Gmitro and Vermeulen and the run with the VLE data of Vermeulen et al., respectively. Successful regression of the run with the VLE data of Bolsaitis and Elliott can only be achieved after we remove the VLE data at 573 K from the regression. Apparently the unusually high water partial pressure data of Bolsaitis and Elliott at high acid concentrations and high temperatures are not consistent and cannot be regressed simultaneously with other available thermodynamic property data in Table 8. With the VLE data at 573 K removed, the regression yields RRMSE of 1.756 for the run with the VLE data of Bolsaitis and Elliott.

While the three runs all achieved acceptable correlation results with most of the property data regressed, the VLE results for the aqueous sulfuric acid solutions are very different. Figures 2a−c show calculated total pressures of the sulfuric acid system based on the three separate regression runs. To validate the model predictions at high temperatures, the total pressure data of Wüster,[20] not included in regression, are also shown in these figures for comparisons. With the VLE data of Gmitro and Vermeulen used in regression, Figure 2a shows the model results match well the Gmitro and Vermeulen total pressure data at 373 K and higher temperatures. Interestingly, as SO_3 mole fraction approaches 0.5, the model would predict total pressures lower than the Gmitro and Vermeulen data at low temperatures, say 273 K, and very close to the Vermeulen et al. data. This finding suggests the Vermeulen et al. data indeed represents a correction to the Gmitro and Vermeulen data. With the VLE data of Vermeulen et al. used in regression, Figure 2b shows the model gives good match to the Vermeulen et al. data set across all temperatures. The total pressure predictions at high temperatures up

dx.doi.org/10.1021/je100930y |J. Chem. Eng. Data 2011, 56, 963–977

to 753 K are in line with the Wüster data up to about 0.98 mass fraction H_2SO_4, as shown in Figure 12a and b. Above 0.98 mass fraction H_2SO_4, the Wüster data seem too high and cannot be matched. The results suggest the Vermeulen data are thermodynamically consistent with all the other thermophysical property data used in the regression. With the VLE data of Bolsaitis and Elliott used in regression and the 573 K data removed, Figure 2c shows the model gives very poor results at low temperatures as SO_3 mole fraction approaches 0.5.

To further validate the model, Figure 13 shows the model predictions for azeotropic concentrations as functions of pressure. While the model predictions based on the VLE data of Gmitro and Vermeulen are reasonable, the model predictions based on the VLE data of Vermeulen et al. yield excellent match to the experimental azeotropic data from Kunzler.[22] No azeotropic concentration predictions can be generated with the model based on the VLE data of Bolsaitis and Elliott.

Given the VLE results shown above, we conclude that the VLE data of Vermeulen et al. are the most reliable and thermodynamically consistent with all the other thermophysical property data used in the regression. We finalize the model parameters and present the model results based on the VLE data of Vermeulen et al. Table 8 summarizes the regression results including the average relative deviation (ARD) percentage of the calculated results from the experimental data. It should be noted that the data of Gmitro and Vermeulen and the data of Bolsaitis and Elliott are not included in the regression for the development of the final model. The ARDs for these two data sources reflect the difference between the estimated data and the model results based on the data of Vermeulen et al. The values for the regressed parameters of this model are given in Tables 2, 3, 9, and 10.

Figure 3 shows the model results for partial pressures of sulfuric acid match well the data of Vermeulen et al. for concentrated sulfuric acid solutions. Figure 3 further shows the Gmitro and Vermeulen data are 1 order of magnitude too high in comparison to the Vermeulen et al. data.

Figure 4 shows the model results for partial pressure of water match well both the data of Vermeulen et al. and the data of Gmitro and Vermeulen for concentrated sulfuric acid solutions. However, upon close examination, the model results for SO_3 concentration approaching 0.5 show better match with the data of Gmitro and Vermeulen and are significantly lower than the data of Vermeulen et al. at low temperatures. This observation suggests the Vermeulen et al. study, while improving the estimations for sulfuric acid partial pressure, probably reported questionable estimates for water partial pressure trending at the limiting condition, i.e., SO_3 mole fraction of 0.5.

As both the Gmitro and Vermeulen study and the Vermeulen et al. study computed SO_3 partial pressures from the water partial pressures and the sulfuric acid partial pressures, we see in Figure 5 that the model results for SO_3 partial pressures at temperatures higher than 573 K closely resemble both the data of the Gmitro and Vermeulen study and the Vermeulen et al. study. At lower temperatures, the model results for SO_3 partial pressure are always lower than the data of the Gmitro and Vermeulen study and the data of the Vermeulen et al. study. Furthermore, the calculated SO_3 partial pressure trending at the limiting case of SO_3 mole fraction of 0.5 is more consistent with the Gmitro and Vermeulen study than with the Vermeulen et al. study.

The calculated degrees of dissociation of the bisulfate ion, $\eta_{HSO_4^-}$, at 298.15 K are compared to the available experimental

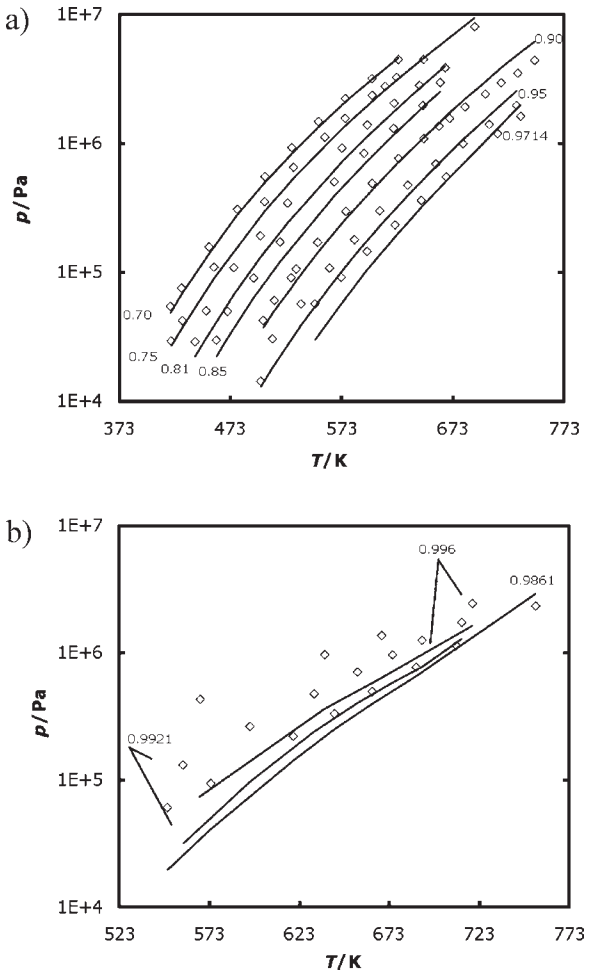

Figure 12. a. Total pressure p of aqueous sulfuric acid system, water (1) + sulfuric acid (2), at mass fractions of apparent sulfuric acid w_2 from 0.7 to 0.9714, versus temperature T. ◇, ref 20; —, model results with model parameters regressed from estimated VLE data of ref 19. b. Total pressure p of aqueous sulfuric acid system, water (1) + sulfuric acid (2), at mass fractions of apparent sulfuric acid w_2 from 0.9861 to 0.996, versus temperature T. ◇, ref 20. —, model results with model parameters regressed from estimated VLE data of ref 19.

data[24−30] in Figure 9. Excellent match in the data trending is obtained using this method.

The model results for the osmotic coefficients at 298.15 K are shown in Figure 10. The model results deviate slightly from the data of Rard et al.[31] at high acid concentrations but match perfectly with the data of Staples[32] across the entire concentration range.

The aqueous phase infinite dilution heat of formation for $H_5O_2^+$ is found to be −574.87 kJ/mol, about twice of that for H_3O^+ (−285.83 kJ/mol). This is reasonable because $H_5O_2^+$ has two water molecules in it and H_3O^+ has one. Figure 11 shows the calculated heat of dilution fits perfectly the experimental data of Wagman et al.[14] Figure 14 shows the model results for heat of mixing at several different temperatures also match well with the experimental data of Kim and Roth.[33] Figure 15 shows the model results match satisfactorily the experimental heat capacity data of Perry's Handbook[35] at 293.15 K for aqueous sulfuric acid solutions. Both the data and the model results exhibit an interesting discontinuity in the slope of Cp vs acid concentration at around 0.80 acid mass fraction (SO_3 apparent mole fraction

dx.doi.org/10.1021/je100930y |J. Chem. Eng. Data 2011, 56, 963–977

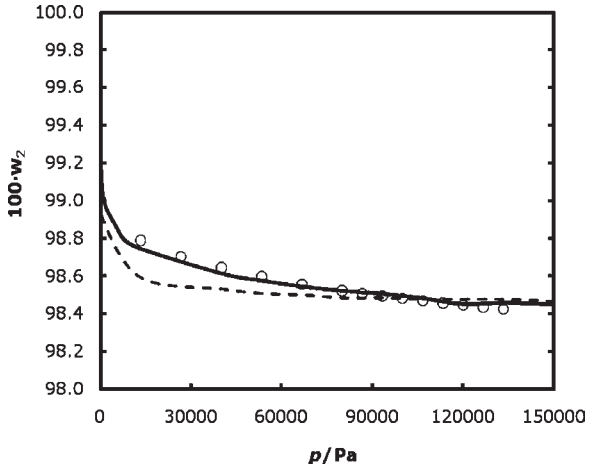

Figure 13. Azeotropic mass percent of apparent sulfuric acid $100 \cdot w_2$ of aqueous sulfuric acid system, water (1) + sulfuric acid (2), versus total pressure p. ○, ref 22; - - -, model predictions with model parameters regressed from estimated VLE data of ref 16; —, model predictions with model parameters regressed from estimated VLE data of ref 19.

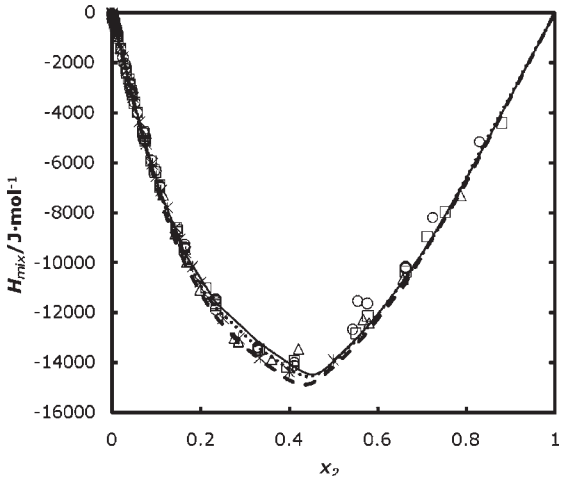

Figure 14. Heat of mixing of aqueous sulfuric acid system, water (1) + sulfuric acid (2), versus mole fraction of apparent sulfuric acid x_2. ○, ref 33; for T = 298.15 K; □, ref 33; for T = 313.15 K; Δ, ref 33; for T = 333.15 K; *, ref 14; for T = 298.15 K; —, model results at T = 298.15 K; ···, model results at T = 313.15 K, ---, model results at T = 333.15 K.

Table 9. Regressed eNRTL Binary Interaction Parameters

component i	component j	$\tau_{1,ij}$	$\tau_{2,ij}$	$\tau_{3,ij}$	α_{ij}
SO_3	H_2SO_4	1.949	−533.53	0.0	0.3
H_2SO_4	SO_3	4.173	−1813.85	0.0	0.3
H_2O	(H_3O^+, HSO_4^-)	6.88	1478.7	−7.954	0.2
(H_3O^+, $HSO4^-$)	H_2O	−4.03	−521.03	3.493	0.2
H_2O	($H_5O_2^+$, HSO_4^-)	6.339	−0.301	−0.118	0.2
($H_5O_2^+$, HSO_4^-)	H_2O	−4.391	−13.292	−0.067	0.2
H_2O	(H_3O^+, SO_4^{-2})	12.238	−0.010	0.229	0.2
(H_3O^+, SO_4^{-2})	H_2O	−4.081	−0.932	0.555	0.2
H_2O	($H_5O_2^+$, SO_4^{-2})	3.494	−0.403	−0.310	0.2
($H_5O_2^+$, SO_4^{-2})	H_2O	−2.442	3.203	0.673	0.2
H_2SO_4	(H_3O^+, HSO_4^-)	3.978	1100.6	−0.062	0.2
(H_3O^+, HSO_4^-)	H_2SO_4	−2.541	−300.97	0.513	0.2
($H_5O_2^+$, HSO_4^-)	($H_5O_2^+$, SO_4^{-2})	5.392	0.0	0.0	0.2
($H_5O_2^+$, SO_4^{-2})	($H_5O_2^+$, HSO_4^-)	−2.465	0.0	0.0	0.2
($H_5O_2^+$, HSO_4^-)	(H_3O^+, HSO_4^-)	−0.115	0.0	0.0	0.2
(H_3O^+, HSO_4^-)	($H_5O_2^+$, HSO_4^-)	0.130	0.0	0.0	0.2

Table 10. Regressed Reaction Equilibrium Constant Parameters

	A	B	ln K @ 298.15 K
R_1	−3.898	3475.0	7.757
R_2	−5.393	1733.1	0.420
R_3	−1.741	853.72	1.122
R_4	−12.29	14245.7	34.49
R_5	−6.307	3122.1	4.165

of ∼ 0.47). This concentration corresponds to the transition of the sulfuric acid system from aqueous sulfuric acid solution to nonaqueous sulfuric acid solution.

As identified by the data regression, the liquid enthalpy of formation at 298.15 K for disulfuric acid is $-1275.0\ kJ \cdot mol^{-1}$ and the liquid heat capacity is $26.934\ J \cdot (mol \cdot K)^{-1}$ at 298.15 K. Liquid heat capacity is treated as constant as we ignore the temperature dependence for this property. With these two parameters, the model correlates well the heat of solution data of liquid SO_3 in H_2SO_4 from Miles et al.,[34] as shown in Figure 16.

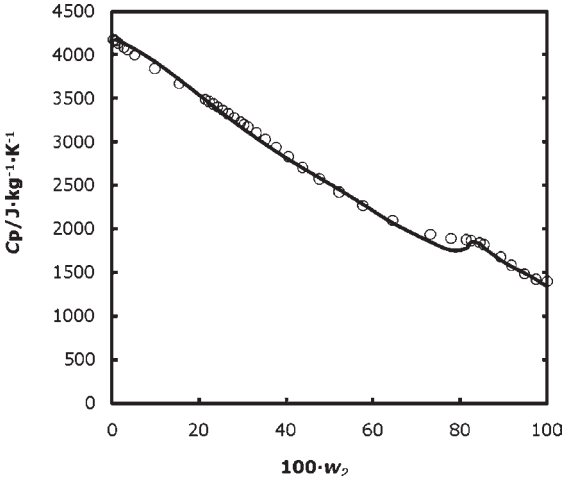

Figure 15. Specific heat capacity Cp of aqueous sulfuric acid system, water (1) + sulfuric acid (2), at T = 293.15 K, versus mass percent of apparent sulfuric acid $100 \cdot w_2$. ○, ref 35; —, model results.

As a further validation of the model, Figure 17 shows a Merkel enthalpy-concentration chart generated for the aqueous sulfuric acid at 101325 Pa. With the exception of some minor differences observed for high sulfuric acid concentrations, the model virtually duplicates the original Merkel chart prepared by McCabe[37] based on the work of Zeisberg[38] for determining the heat required for concentrating sulfuric acid solutions. Note that the Merkel chart makes use of the English unit. The standard state of the acid is taken to be pure acid at 70 °F. The chart covers the temperature range from 70 °F to the atmospheric boiling point. Given that the model correlates well the comprehensive set of

dx.doi.org/10.1021/je100930y |J. Chem. Eng. Data 2011, 56, 963–977

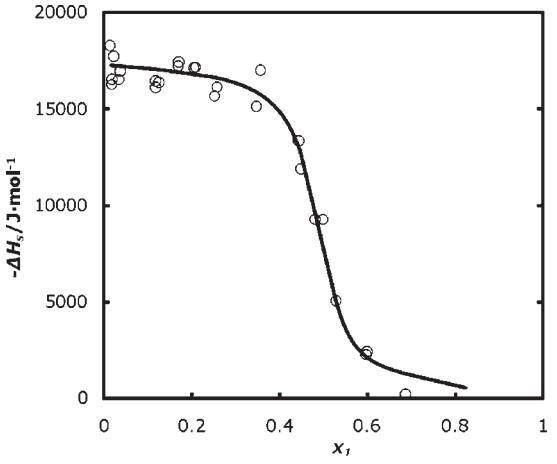

Figure 16. Heat of solution ΔH_s of liquid sulfur trioxide (1) in sulfuric acid (2), at $T = 303.15$ K, versus mole fraction of apparent sulfur trioxide x_1. ○, ref 34; —, model results.

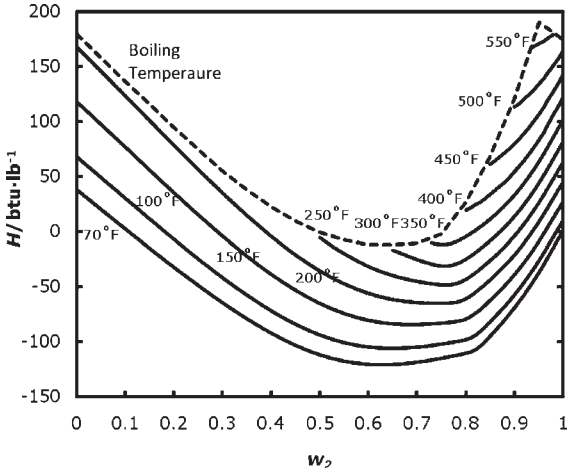

Figure 17. Merkel enthalpy-concentration chart for aqueous sulfuric acid system, enthalpy H of aqueous sulfuric acid system, water (1) + sulfuric acid (2), at $p = 101325$ Pa from room temperature to boiling temperatures, versus mass fraction of apparent sulfuric acid w_2. —, model results.

relevant thermophysical property data summarized in Table 8, Figure 17 can be considered as an update to McCabe's Merkel enthalpy-concentration chart for sulfuric acid solutions.

Separately, the compositions of the species at 298.15 K in the sulfuric acid system are shown in Figure 18. It shows $H_5O_2^+$ is the major hydrated proton species in dilute sulfuric acid solution while H_3O^+ becomes the dominant one in more concentrated sulfuric acid solution. Sulfate ion is always of low concentration in comparison to bisulfate ion, due to the relative weakness of the second acid dissociation. With the increase in SO_3 mole fraction, water concentration diminishes rapidly as water is consumed by the dissociation of sulfuric acid and the hydrations of proton ion. As SO_3 mole fraction exceeds ~ 0.47, hydronium ion and bisulfate ion concentrations drop precipitously and the solution transitions to mainly nonaqueous sulfuric acid. Further increase of SO_3 brings about the reaction between sulfuric acid and sulfur trioxide to form a nonaqueous mixture of sulfuric acid, sulfur trioxide, and disulfuric acid.

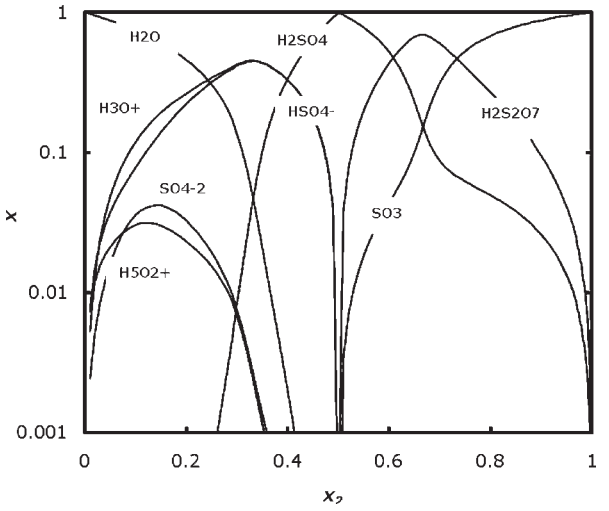

Figure 18. Mole fractions of true species x in the sulfuric acid system, water (1) + sulfur trioxide (2), at $T = 298.15$ K, versus mole fraction of apparent sulfur trioxide x_2. —, model results.

CONCLUSIONS

The complexity of the sulfuric acid−water−sulfur trioxide system presents a tall challenge to the development of thermodynamic model for the sulfuric acid system. Based on the symmetric eNRTL activity coefficient model, we have developed an accurate and comprehensive thermodynamic model for the sulfuric acid system that covers the entire concentration range from pure water, to pure sulfuric acid, to pure sulfur trioxide. The model satisfactorily represents all the relevant thermophysical property data including vapor−liquid equilibrium, osmotic coefficients, liquid phase speciation, heat of dilution, heat of mixing, and liquid heat capacity with temperature ranging from room temperature up to 773 K. It should be a very useful engineering thermodynamic model in support of modeling and simulation of processes involving the sulfuric acid system.

AUTHOR INFORMATION

Corresponding Author

*E-mail: chauchyun.chen@aspentech.com. Phone: 781-221-6420. Fax: 781-221-6410.

ACKNOWLEDGMENT

We thank M. B. Gorensek, R. Field, P. M. Mathias, L. Brown, G. M. Bollas, and J. DeVincentis for helpful discussions.

REFERENCES

(1) Gorensek, M. B.; Edwards, T. B. Energy Efficiency Limits for a Recuperative Bayonet Sulfuric Acid Decomposition Reactor for Sulfur Cycle Thermochemical Hydrogen Production. *Ind. Eng. Chem. Res.* **2009**, *48*, 7232–7245.

(2) Chen, C.-C.; Mathias, P. M. Applied Thermodynamics for Process Modeling. *AIChE J.* **2002**, *48*, 194–200.

(3) Bollas, G. M.; Chen, C.-C.; Barton, P. I. Refined Electrolyte-NRTL Model: Activity Coefficient Expressions for Application to Multi-Electrolyte Systems. *AIChE J.* **2008**, *54*, 1608–1624.

(4) Wang, P.; Anderko, A.; Springer, R. D.; Young, R. D. Modeling Phase Equilibria and Speciation in Mixed-Solvent Electrolyte Systems: II. Liquid-Liquid Equilibria and Properties of Associating Electrolyte Solutions. *J. Mol. Liq.* **2006**, *125*, 37–44.

(5) Clegg, S. L.; Brimblecombe, P. Application of a Multicomponent Thermodynamic Model to Activities and Thermal Properties of 0−40 mol kg^{-1} Aqueous Sulfuric Acid from <200 to 328 K. *J. Chem. Eng. Data* **1995**, *40*, 43–64.

(6) Song, Y.; Chen, C.-C. Symmetric Electrolyte Nonrandom Two-Liquid Activity Coefficient Model. *Ind. Eng. Chem. Res.* **2009**, *48*, 7788–7797.

(7) Chen, C.-C.; Britt, H. I.; Boston, J. F.; Evans, L. B. Local Composition Model for Excess Gibbs Energy of Electrolyte Systems. Part I: Single Solvent, Single Completely Dissociated Electrolyte Systems. *AIChE J.* **1982**, *28*, 588–596.

(8) Chen, C.-C.; Mathias, P. M.; Orbey, H. Use of Hydration and Dissociation Chemistries with the Electrolyte-NRTL Model. *AIChE J.* **1999**, *45*, 1576–1586.

(9) Borman, S. Revisiting the Hydrated Proton. *Chem. Eng. News* **2005**, *83* (27), 26–27.

(10) Headrick, J. M.; Diken, E. G.; Walters, R. S.; Hammer, N. I.; Christie, R. A.; Cui, J.; Myshakin, E. M.; Duncan, M. A.; Johnson, M. A.; Jordan, K. D. Spectral Signatures of Hydrated Proton Vibrations in Water Clusters. *Science* **2005**, *308*, 1765–1769.

(11) Nilges, J.; Schrage, J. Vapor-Liquid Equilibrium of the System H_2SO_4-SO_3. Part II. Thermodynamic Description with regard to the Formation of $H_2S_2O_7$. *Fluid Phase Equilib.* **1991**, *68*, 247–261.

(12) Schrage, J. Vapor-Liquid Equilibrium of the System H_2SO_4-SO_3. Part I. Vapor Pressure Measurements with a New Static Vapor Pressure Apparatus. *Fluid Phase Equilib.* **1991**, *68*, 229–245.

(13) *Aspen Physical Property System, v7.2*; Aspen Technology, Inc.: Burlington, MA., 2010.

(14) Wagman, D. D.; Evans, W. H.; Parker, V. B.; Schumm, R. H.; Halow, I.; Bailey, S. M.; Churney, K. L.; Nuttall, R. L. The NBS Tables of Chemical Thermodynamic Properties - Selected Values for Inorganic and C1 and C2 Organic Substances in SI Units. *J. Phys. Chem. Ref. Data* **1982**, 11Supplement No. 2. Pages 2−57 to 2−59.

(15) Maryott, A. A.; Smith, E. R. *Table of Dielectric Constants of Pure Liquids*; National Bureau of Standards: Gaithersburg, MD, 1951; p 4.

(16) Gmitro, J. I.; Vermeulen, T. Vapor-Liquid Equilibria for Aqueous Sulfuric Acid. *AIChE J.* **1964**, *10*, 740–746.

(17) Roedel, W. Measurement of Sulfuric Acid Saturation Vapor Pressure; Implications for Aerosol Formation by Heteromolecular Nucleation. *J. Aerosol Sci.* **1979**, *10*, 375–386.

(18) Ayers, G. P.; Gillett, R. W.; Gras, J. L. On the Vapor Pressure of Sulfuric Acid. *Geophys. Res. Lett.* **1980**, *7*, 433–436.

(19) Vermeulen, T.; Dong, J.; Robinson, S.; Nguyen, T., Vapor-Liquid Equilibrium of the Sulfuric Acid-Water System. *AIChE Meeting.*, 1982, Anaheim, CA .

(20) Wüster, G., *P, v, T - und Dampfdruckmessungen zur Bestimmung Thermodynamischer Eigenschaften Starker Elektrolyte bei Erhöhtem Druck", Doctoral Dissertation*, RWTH Aachen University, Aachen, Germany, 1979.

(21) Bolsaitis, P.; Elliott, J. F. Thermodynamic Activities and Equilibrium Partial Pressures for Aqueous Sulfuric-Acid-Solutions. *J. Chem. Eng. Data* **1990**, *35*, 69–85.

(22) Kunzler, J. E. Absolute Sulfuric Acid, a Highly Accurate Primary Standard. *Anal. Chem.* **1953**, *25*, 93–103.

(23) Lindstrom, R. E.; Wirth, H. E. Estimation of the Bisulfate Ion Dissociation in Solutions of Sulfuric Acid and Sodium Bisulfate. *J. Phys. Chem.* **1969**, *73*, 218–223.

(24) Young, T. F.; Maranville, L. F.; Smith, H. M. *The Structure of Electrolytic Solutions*; Wiley: New York, 1959; pp 35−63.

(25) Sherrill, M. S.; Noyes, A. A. The Inter-ionic Attraction Theory of Ionized Solutes VI. The Ionization and Ionization Constants of Moderately Ionized Acids. *J. Am. Chem. Soc.* **1926**, *48*, 1861–1873.

(26) Chen, H.; Irish, D. E. A Raman Spectral Study of Bisulfate-Sulfate Systems. II. Constitution, Equilibria, and Ultrafast Proton Transfer in Sulfuric Acid. *J. Phys. Chem.* **1971**, *75*, 2672–2681.

(27) Librovich, N. B.; Maiorov, V. D. Ionic-Molecular Composition of Aqueous Sulfuric-Acid Solutions at 25°. *Bull. Acad. Sci. USSR Div. Chem. Sci.* **1977**, *26*, 621–623.

(28) Hood, G. C.; Reilly, C. A. Ionization of Strong Electrolytes. V. Proton Magnetic Resonance in Sulfuric Acid. *J. Chem. Phys.* **1957**, *27*, 1126–1128.

(29) Myhre, C. E. L.; Christensen, D. H.; Nicolaisen, F. M.; Nielsen, C. J. Spectroscopic Study of Aqueous H_2SO_4 at Different Temperatures and Compositions: Variations in Dissociation and Optical Properties. *J. Phys. Chem. A* **2003**, *107*, 1979–1991.

(30) Rard, J. A.; Habenschuss, A.; Spedding, F. H. A Review of the Osmotic Coefficients of Aqueous H_2SO_4 at 25 °C. *J. Chem. Eng. Data* **1976**, *21*, 374–379.

(31) Staples, B. R. Activity and Osmotic Coefficients of Aqueous Sulfuric Acid at 298.15 K. *J. Phys. Chem. Ref. Data* **1981**, *10*, 779–798.

(32) Rütten, P.; Kim, S. H.; Roth, M. Measurements of the Heats of Dilution and Description of the System H_2O/H_2SO_4/HCl with a Solvation Model. *Fluid Phase Equilib.* **1998**, *153*, 317–340.

(33) Kim, S. H.; Roth, M. Enthalpies of Dilution and Excess Molar Enthalpies of an Aqueous Solution of Sulfuric Acid. *J. Chem. Eng. Data* **2001**, *46*, 138–143.

(34) Miles, F. D.; Niblock, H.; Smith, D. The Heat of Formation of Oleum. *Trans. Faraday. Soc.* **1944**, *40*, 281–295.

(35) *Perry's Chemical Engineers' Handbook*, 8th ed.; Green, D. W., Perry, R. H., Eds.; McGraw-Hill: New York, 2008; pp 2−184.

(36) Bodenstein, M.; Katayama, M. Die Dissociation von Hydratischer Schefelsaure und von Stickstoffdioxyd. *Z. Elektrochem.* **1909**, *15*, 244–249.

(37) McCabe, W. L. The Enthalpy-Concentration Chart - A Useful Device for Chemical Engineering Calculations. *Trans. Am. Inst. Chem. Eng.* **1935**, *31*, 129–164.

(38) Zeisberg, F. C. Thermal Considerations in Sulphuric Acid Concentration. *Trans. Am. Inst. Chem. Eng.* **1922**, *14*, 1–11.